Developmental Biology 352 (2011) 116–127

Contents lists available at ScienceDirect

Developmental Biology

journal homepage: www.elsevier.com/developmentalbiology

Altered differentiation and paracrine stimulation of mammary epithelial cell proliferation by conditionally activated Smoothened

Adriana P. Visbal [a], Heather L. LaMarca [b], Hugo Villanueva [b,c], Michael J. Toneff [b,c], Yi Li [b,c], Jeffrey M. Rosen [a,b], Michael T. Lewis [a,b,c,*]

[a] Program in Developmental Biology Baylor College of Medicine, One Baylor Plaza, Houston, TX 77030, USA
[b] Department of Molecular and Cellular Biology, Baylor College of Medicine, One Baylor Plaza, Houston, TX 77030, USA
[c] Lester and Sue Smith Breast Center, Baylor College of Medicine, One Baylor Plaza, Houston, TX 77030, USA

ARTICLE INFO

Article history:
Received for publication 11 September 2010
Revised 14 January 2011
Accepted 19 January 2011
Available online 27 January 2011

Keywords:
SmoM2
Ductal hyperplasia
Paracrine tissue interactions
Hedgehog signaling
Microenvironment
Notch signaling

ABSTRACT

The Hedgehog (Hh) signaling network is critical for patterning and organogenesis in mammals, and has been implicated in a variety of cancers. Smoothened (Smo), the gene encoding the principal signal transducer, is overexpressed frequently in breast cancer, and constitutive activation in MMTV-SmoM2 transgenic mice caused alterations in mammary gland morphology, increased proliferation, and changes in stem/progenitor cell number. Both in transgenic mice and in clinical specimens, proliferative cells did not usually express detectable Smo, suggesting the hypothesis that Smo functioned in a non-cell autonomous manner to stimulate proliferation. Here, we employed a genetically tagged mouse model carrying a Cre-recombinase-dependent conditional allele of constitutively active Smo (SmoM2) to test this hypothesis. MMTV-Cre- or adenoviral-Cre-mediated SmoM2 expression in the luminal epithelium, but not in the myoepithelium, was required for the hyper-proliferative phenotypes. High levels of proliferation were observed in cells adjacent or in close-proximity to Smo expressing cells demonstrating that SmoM2 expressing cells were stimulating proliferation via a paracrine or juxtacrine mechanism. In contrast, Smo expression altered luminal cell differentiation in a cell-autonomous manner. SmoM2 expressing cells, purified by fluorescence activated cell sorting (FACS) via the genetic fluorescent tag, expressed high levels of Ptch2, Gli1, Gli2, Jag2 and Dll-1, and lower levels of Notch4 and Hes6, in comparison to wildtype cells. These studies provide insight into the mechanism of Smo activation in the mammary gland and its possible roles in breast tumorigenesis. In addition, these results also have potential implications for the interpretation of proliferative phenotypes commonly observed in other organs as a consequence of hedgehog signaling activation.

Introduction

The Hedgehog (Hh) signaling network plays essential roles in patterning and organogenesis during metazoan development. In mammals, Hh signaling regulates morphogenesis, cell fate, and stem/progenitor cell maintenance, and functions in virtually every organ and structure in the body, including the mammary gland (Jia and Jiang, 2006; McMahon et al., 2003). Mutations in several Hh network genes, or deregulated network activity, have been implicated in the development of a variety of cancers including those of the skin, lung, pancreas, gastrointestinal system, prostate, and breast (reviewed in (Chari and McDonnell, 2007; Evangelista et al., 2006; Kasper et al., 2009; Varjosalo and Taipale, 2008; Visbal and Lewis, 2010).

Mammary gland development is a highly regulated process governed by both systemic hormones and local growth factors- and adhesion-mediated epithelial–stromal and epithelial–epithelial cell interactions. Development in virgin animals is largely limited to ductal elongation and branching morphogenesis, as well as differentiation of the luminal and myoepithelial cell types present in the mature virgin ducts (Watson and Khaled, 2008). While limited alveolar development does occur in virgin mammals in some species (e.g. humans), functional differentiation of the mammary gland does not occur until pregnancy and lactation with the development of secretory alveolar structures and milk production.

Our work and the work of others have demonstrated key roles for selected Hh network genes in mediating epithelial–stromal interactions in virgin mice. While no mammary functions have been ascribed to any of the three Hh ligands, Patched-1 (Ptch1), which acts as an inhibitor of network signaling in the absence of a hedgehog ligand, and as a signal transducing receptor in their presence, is required in both the epithelium and the mammary stroma (as well as systemically) for normal ductal morphogenesis (Moraes et al., 2009). Gli2, a

* Corresponding author at: Lester and Sue Smith Breast Center, Baylor College of Medicine, One Baylor Plaza, Houston, TX 77030, USA.
E-mail address: mtlewis@bcm.edu (M.T. Lewis).

0012-1606/$ – see front matter © 2011 Elsevier Inc. All rights reserved.
doi:10.1016/j.ydbio.2011.01.025

key transcriptional factor regulating hedgehog target gene expression is also required in the mammary stroma for proper duct patterning (Lewis et al., 2001). In addition to these loss-of-function studies, overexpression analyses in transgenic mice have shown defects in mammary gland morphology and altered stem/progenitor cell number in mice expressing constitutively activated Smoothened (Smo), the Hh pathway's main signal transducer (Moraes et al., 2007). Additionally, lactation defects and tumor formation in multiparous mice were observed in transgenic animals expressing the Gli1 transcription factor (Fiaschi et al., 2009; Fiaschi et al., 2007).

In previous studies from our laboratory, we demonstrated that Smo is frequently ectopically expressed in human breast cancers, particularly in ductal carcinoma *in situ* (DCIS), an early breast cancer lesion. About seventy percent of DCIS lesions, and about thirty percent of invasive breast cancers (IBC), showed ectopic expression relative to normal mammary epithelium in which expression was not detectable (Moraes et al., 2007). Consistent with a potential role in breast cancer, expression of a constitutively activated form of Smo (SmoM2) under the control of the mouse mammary tumor virus (MMTV) promoter indicated that Smo activation in a small percentage (~5%) of luminal mammary epithelial cells led to increased proliferation and abnormal ductal morphology of the mammary gland (Moraes et al., 2007). Both in transgenic mice and in clinical specimens, proliferative cells did not usually express detectable Smo, suggesting the possibility that Smo functioned in a non-cell autonomous paracrine or juxtacrine manner to stimulate proliferation. In both Ptch1 loss-of-function and MMTV-SmoM2 mice (both mutations generally leading to ectopic signaling), there was no evidence that canonical Gli-mediated Hh signaling was active, as evidenced by lack of increased expression of autoregulated network genes (e.g. Ptch1, Gli1, Gli2). Thus, both the cellular and molecular mechanisms underlying the effects of abnormal Smo expression in the mouse or human mammary gland remained unclear.

In this study, we took advantage of a conditional knock-in mouse model that allows expression of a SmoM2–YFP fusion protein upon Cre-mediated recombination under the control of the endogenous Rosa26 promoter to increase the percentage of cells expressing SmoM2. Additionally, we employed a dual fluorescent Cre-responsive reporter line that allowed us to genetically tag SmoM2 expressing cells and distinguish them from wild type cells. The use of these models allowed us to differentiate whether the effects of Smo activation were cell-autonomous, or whether they were being mediated by a paracrine/juxtacrine mechanism. Additionally, fluorescently tagged cells could be purified using fluorescence activated cell sorting (FACS) to examine the activation state of the hedgehog network in Smo expressing cells relative to the surrounding wildtype cells.

Materials and methods

Mouse strains and breeding

The previously described R26SmoM2, herein referred to as SmoM2, and the dual fluorescence mT-mG Cre-recombinase reporter mouse lines (Fig. S1) were obtained from Jackson Laboratories (stock numbers 005130 and 007576, respectively) and maintained in a mixed genetic background (Jeong et al., 2004; Muzumdar et al., 2007). The MMTV-Cre (Li et al., 2002) and R26R Cre-dependent LacZ reporter (Soriano, 1999) lines were generous gifts from T. Lane (UCLA, Los Angeles, CA) and P. Soriano (Fred Hutchinson Cancer Research Center, Seattle, WA), respectively. For our initial studies in which the epithelium was not genetically tagged with a Cre reporter, F1 SmoM2/+; MMTV-Cre and SmoM2/+ littermates were used. For some subsequent transplantation experiments, SmoM2/SmoM2 mice were crossed to R26R/R26R animals to create a genetically tagged line expressing LacZ in cells undergoing Cre-mediated recombination. For experiments in which the epithelium was tagged with a fluorescent reporter, the SmoM2 line was backcrossed four generations into FVB and then intercrossed to produce SmoM2/SmoM2 homozygotes. The resulting homozygous mice were subsequently crossed to MMTV-Cre/+;mT-mG/mT-mG mice. The resulting SmoM2/mT-mG; Cre + mice allowed for recombined cells expressing the SmoM2 transgene to be tagged with EGFP while surrounding cells that did not undergo recombination to remain labeled with TomatoRed. Immunocompromised SCID/beige mice purchased from Charles River (Houston, TX) were used as transplantation hosts. Genotyping of mice was carried out by allele-specific PCR using primers listed in Supplemental Table S1. All animals were maintained in accordance with the NIH Guide for the Care and Use of Experimental Animals with approval from the Baylor College of Medicine Institutional Animal Care and Use Committee.

Tissue harvesting and processing

In intact mice, mammary glands were harvested at 5, 7, 9 and 10 weeks of age. Two hours prior to tissue harvest, animals were injected with 10 μl/gram of body weight of bromodeoxyuridine (BrdU) (3 mg/ml) in PBS to allow evaluation of proliferation. Vaginal smears were used, along with the appearance of the vagina and uterus, to determine the stage of estrus cycle upon harvest.

For whole gland imaging, the #1, 3, 4, and 5 mammary glands from the left side of the animal were collected and processed for whole mount preparations. For gene expression analysis, the #1, 3, 4 (without the lymph node), and 5 mammary glands from the right side of the animal were frozen in liquid nitrogen for subsequent protein, RNA, and DNA extraction.

Primary mammary epithelial cell isolation and FACS analysis

For yellow fluorescent protein (YFP) detection by fluorescence activated cell sorting (FACS) analysis, freshly isolated mammary epithelial cells (MECs) from individual mice (at least 3 Cre+ and 3 Cre− animals either 9 or 10 weeks of age) were derived from #1, #3, #4 (without the lymph node) and #5 mammary glands. The glands were then minced into 1 mm^3 fragments using a Vibratome Series 800-Mcllwain Tissue Chopper (Vibratome, St. Louis, MO) and digested in 2 mg/ml collagenase A (Roche Applied Science, Indianapolis, IN) in F12 Nutrient Mixture containing 1× antibiotic–antimycotic (InVitrogen, Carlsbad, CA) for 1 h at 37 °C with shaking at 200 rpm. Single cells were purified as described previously (Welm et al., 2008). Single cells were resuspended in HBSS containing 2% FBS and 10 mM HEPES buffer, filtered through a 40 μm cell strainer, and stained with SytoxRed (InVitrogen) to exclude dead cells. Samples were analyzed for YFP fluorescence using an LSRII Analyzer (BD Biosciences, San Jose, CA).

Adenovirus transduction and transplantation

For conditional overexpression experiments, freshly isolated MECs were incubated with an adenovirus expressing Cre recombinase (Ad-Cre) to induce recombination (Rijnkels and Rosen, 2001) at a multiplicity of infection of 50 in 2 ml of 5% FBS/DMEM F12 for 1 h at 37 °C in suspension. The cells were then centrifuged at 450×*g* for 5 min, washed with 5 ml of 5% FBS/DMEM-F12, and resuspended to 25,000 cells/μl in a 1:1 solution of PBS and Matrigel (BD Biosciences), on ice until transplantation (Moraes et al., 2007). Cells (250,000/fat pad) were injected into contralateral cleared fat pads of SCID/Beige host mice as described previously (Deome et al., 1959). After 8 weeks, mammary glands were harvested and processed for whole-gland and histological analysis.

Whole-mount analysis and X-gal staining

For untagged mammary glands, SmoM2;+ and SmoM2;MMTV-Cre animals, the #4 mammary glands were harvested, fixed in ice cold 4% paraformaldehyde for 2 h, and stained with hematoxylin as described previously (Daniel et al., 1989). At least ten Cre+ and Cre− animals were analyzed, and three mice of each genotype were used for quantification of branching. Briefly, ten 4× fields were imaged per gland on a Leica MZ16F fluorescent stereoscope (Meyer Instruments, Houston, TX) and all branches counted.

For experiments in which the epithelium was genetically tagged with the R26R LacZ reporter, after transplantation, contralateral #4 mammary glands (and a host #3 gland as an endogenous control) were fixed as described above for 1 h and washed three times for 30 min in wash buffer containing 0.2% NP-40, 0.01% sodium deoxycholate, and 2 mM magnesium chloride in 1× PBS. Glands were then pre-incubated in wash buffer containing 25 mM potassium ferrocyanide and 25 mM potassium ferricyanide for 1 h at 37 °C and stained overnight in the above solution containing 1 mg/ml X-gal (InVitrogen). Glands were then dehydrated in a series of 70%, 95% and 100% ethanol and imaged. All glands were then embedded in paraffin for further histological analysis.

For fluorescence imaging of whole mount preparations (Landua et al., 2009) mammary glands 1–5 on the left side of the animal, as well as salivary gland, uterus and ovaries were harvested, placed onto a 6-well dish and left in 50% glycerol/PBS rocking overnight at 4 °C. The next day, tissues were flattened between two glass slides and imaged using a Leica MZ16F microscope (Meyer Instruments). Tissues were then fixed as described above and paraffin embedded.

Intraductal adenovirus delivery

Adenovirus-Cre and adenovirus-LacZ were diluted to 1^{10} pfu/ml in Ringer's solution containing bromophenol blue as a marker dye. Inguinal and thoracic mammary glands of three 6.5 wk old SmoM2/mTmE mice were injected with 10 µl of Ad-Cre virus (right side) or Ad-LacZ virus (left side) as previously described (Russell et al., 2003). Mammary glands were harvested two weeks after injection.

FACS sorting and RNA Isolation and Amplification

MECs from Cre+ and Cre+ SmoM2/mTmE 10 wk old mice were isolated as described above and stained with a lineage panel cocktail to exclude non-epithelial cells as previously described (LaMarca et al., 2010). SmoM2;+, SmoM2;Cre (Tomato red), and SmoM2;Cre (EGFP) cells were then sorted into wildtype Red, Cre Red, and Cre Green populations by FACS using an AriaII instrument (BD Biosciences). Total RNA was subsequently isolated using a Qiagen miRNeasy kit, according to the manufacturer's instructions (Qiagen). RNA was then analyzed for quality control and cDNA was generated and amplified using a NuGEN WT-Ovation RNA Amplification kit according to the manufacturer's instructions (NuGEN).

Immunostaining

Five to seven µm sections were deparaffinized and re-hydrated to PBS through a graded series of ethanols. Heat-induced antigen retrieval was performed in 10 mM sodium citrate by boiling for 20 min. All washes were performed with PBS and primary antibodies were incubated at 4 °C overnight. BrdU (1:10, BD Biosciences) and NKCC1 (1:200, kind gift from Dr. Kim Turner, NIH, Bethesda, MD) were diluted in 5% BSA, 0.5% Tween blocking buffer, and keratin 8 (K8; 1:200, Developmental Studies Hybridoma Bank, University of Iowa), K14 (1:200 Covance, Princeton, NJ), EGFP (1:1000, InVitrogen), and F4/80 (1:200, InVitrogen) were diluted in M.O.M block (Vector Laboratories, Burlingame, CA). For immunohistochemistry (BrdU, F4/80), Vectastain Elite ABC and diaminobenzidine (DAB) substrate kits (Vector Laboratories) were used according to the manufacturer's instructions. Following detection, sections were counterstained with hematoxylin, and slides coverslipped using Permount (Fisher). Images were captured using an Olympus BX-40 microscope (Leeds Instruments, Irving, TX). BrdU-positive cells were counted using ImagePro Plus 6.1 software (Media Cybernetics, Bethesda, MD) (five 40× fields per section, two sections per gland, at least 4 glands for each genotype). For immunofluorescence, slides were washed with PBS and incubated with AlexaFluor (InVitrogen) secondary antibodies (1:200) for 1 h at room temperature, washed in PBS and then mounted in Vectashield with DAPI (Vector Laboratories).

Quantitative RT-PCR (qPCR)

Total RNA from # 4 mammary glands (after lymph node removal) was isolated using Trizol Reagent (InVitrogen) according to the manufacturer's instructions. RNA samples were then DNase-treated (InVitrogen) and cDNA was synthesized using Superscript III RT kit (InVitrogen) according to the manufacturer's protocol. For FACS sorted cells RNA was isolated and amplified as described above. qPCR was performed using ABI reagents and Taqman Probe and Primer Sets (assay ID numbers found in Supplemental Table S2) or SYBRgreen (Applied Biosystems, Foster City, CA) and were normalized to 18S ribosomal RNA or ß-actin, respectively. All qPCR was performed using the StepOnePlus Real-Time PCR System (Applied Biosystems). Relative levels of expression were calculated using the ΔΔCt method using Cre-negative litter-mates or Wildtype SmoM2;+ populations as calibrators (Livak and Schmittgen, 2001).

Statistical analysis

Data from branching quantitation and BrdU incorporation are presented as the means ± standard error of the means (SEM). SmoM2;Cre glands were compared to SmoM2;+ glands and the differences were analyzed using an unpaired Student's *t*-test (GraphPad Prism© Home, San Diego, CA.) For gene expression studies differences in relative quantitation were analyzed using a paired Student's *t*-test.

Results

Previous analysis of mammary glands from an MMTV-SmoM2 transgenic mouse showed increased proliferation, and ductal hyperplasia in virgin mice. In this model, SmoM2 expression was driven by the MMTV-LTR in a small percentage of mammary epithelial cells. To ensure that similar changes also occurred in the Cre-dependent conditional model in which SmoM2 was knocked into the ROSA locus, we harvested mammary glands from SmoM2;+ (wild type) and SmoM2;Cre (SmoM2 expressing) animals at 5, 7, 9 and 10 weeks of age and analyzed for overall morphology. Consistent with previous results using MMTV-SmoM2 mice, at 5 weeks of age there was a significant increase in the number of terminal end buds (TEBs), the highly proliferative structures that drive ductal morphogenesis in SmoM2;Cre mice relative to Cre-negative controls (Fig. 1A,B). Accelerated ductal outgrowth was apparent at 7 weeks of age when the ductal epithelia from SmoM2;Cre animals reached the end of the fat pad, in contrast to the ducts from Cre-negative littermates (SmoM2;+) (Fig. 1A). At 9 weeks of age, ductal epithelia from both Cre-positive (SmoM2;Cre) and Cre-negative (SmoM2;+) animals completely filled the fat pad, and were morphologically indistinguishable from one another (Fig. 1A). By flow cytometric analysis, approximately 45% (44.7 ± 12.78%) of MECs from Cre-positive animals expressed the SmoM2-YFP fusion protein (Fig. 1 C).

Whereas glands in SmoM2;Cre and SmoM2;+ mice were indistinguishable at 9 weeks of age, a dramatic phenotypic transition occurred at 10 weeks of age. Glands from SmoM2;Cre animals

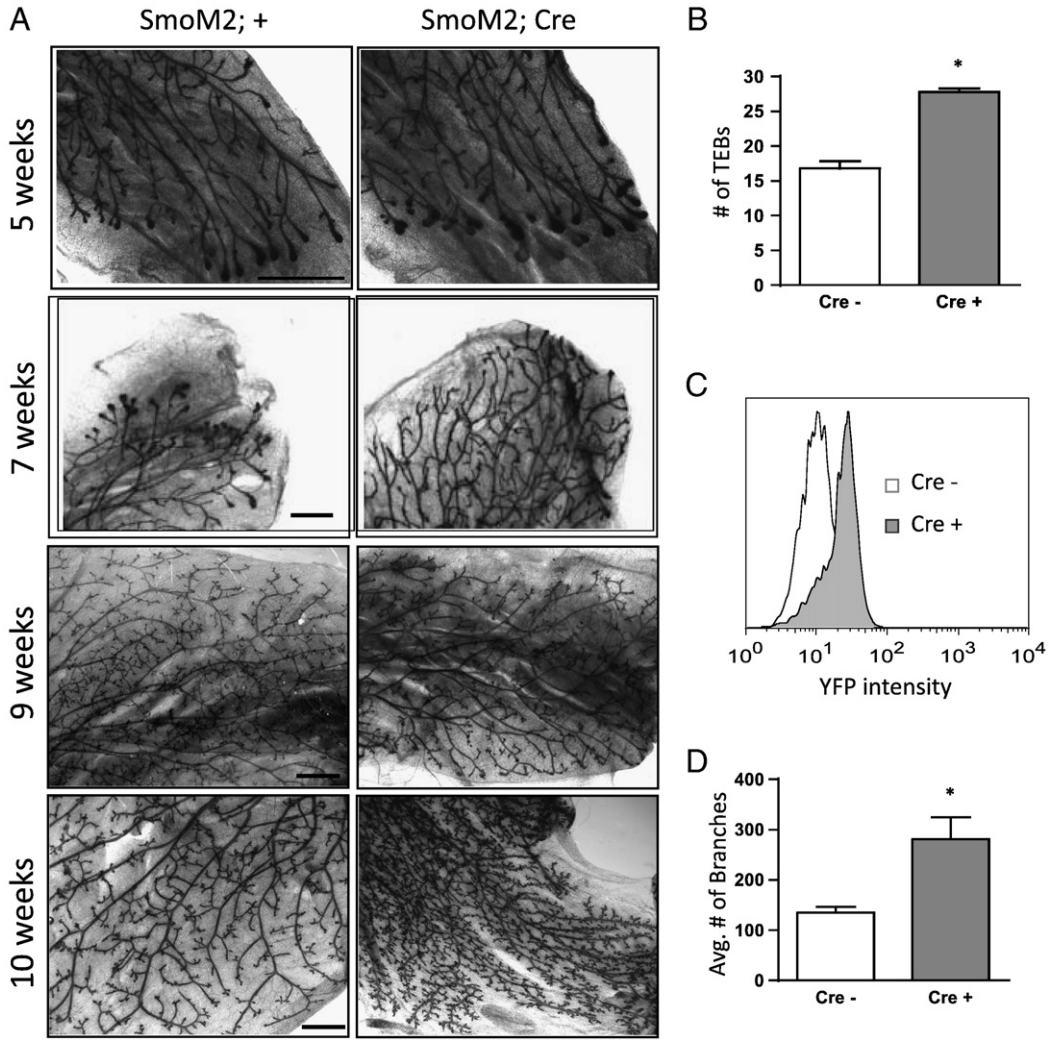

Fig. 1. SmoM2 expression leads to increased number of TEBs and hyper-branching of the mammary gland. Hematoxylin stained whole-mounts of mammary glands from SmoM2;+ or SmoM2;Cre animals at 5, 7, 9 and 10 weeks of age. Cre positive animals exhibit a significant increase in number of TEBs at 5 weeks ($p<0.01$) (B) as well number of branches at 10 weeks ($p=0.03$) (D) as compared to their Cre negative litter-mates. At 7 weeks of age mammary glands from Cre positive animals have reached the end of the fat pad whereas their Cre-negative litter-mates have not. At 9 weeks of age, SmoM2;+ and SmoM2;Cre mammary glands are morphologically indistinguishable. FACS analysis for SmoM2-YFP fusion at 9 weeks showing that approximately 45% of MECs express YFP (C). Scale bars A,B: 5 mm D,E,G,H: 5 mm.

showed a significant increase ($p<0.01$) in the number of branches along the mammary ductal tree compared to Cre-negative littermates (Fig. 1A and D). Additionally, alveolar bud-like structures were observed throughout the Cre-positive mammary glands that were reminiscent of alveolar development normally observed during pregnancy. To ensure that this phenotypic change was not simply due to a change in the percentage of cells expressing SmoM2-YFP, we repeated the FACS analysis. Again, approximately 50% ($52.2\pm2.3\%$) of the MECs from SmoM2;Cre mice expressed the SmoM2-YFP protein (Fig. S2).

To determine if the morphological and developmental changes observed were associated with increased proliferation, immunostaining for BrdU incorporation was used as an indicator for cells in S phase. At 5 weeks of age, we observed a significant increase in BrdU incorporation in the TEBs of Cre-positive mammary glands relative to Cre-negative glands (Fig. 2A vs. 2B,C). At 9 weeks of age, the Cre-negative animals exhibit low levels of proliferation in the mammary gland, characteristic of the mature virgin state (Fig. 2D), whereas Cre-positive animals showed a significant increase in the number of proliferating cells (Fig. 2E,F). Unexpectedly, at 10 weeks of age, there was no difference in proliferation between SmoM2;Cre and SmoM2;+ mice (Fig. 2G–I), with ductal epithelium showing approximately 2% BrdU positive cells.

Epithelial SmoM2 expression disrupts histoarchitecture, increases periductal collagen deposition, and increases macrophage recruitment

Histological examination of mammary gland sections from 10-week-old mice revealed the presence of alveolar-like structures in the Cre-positive mammary glands as compared to controls (Fig. 3A,B). Cre-positive mammary glands also exhibited dissociation of the luminal and myoepithelial cell layers, and luminal cells had an enlarged, clear cytoplasm as compared to Cre-negative littermates. Additionally, the periductal stroma surrounding the hyper-branched Cre-positive 10-week old mammary glands was thickened with an increase in stromal cellularity. In order to characterize the thickened stroma, Masson's Trichrome staining was performed, which revealed an increase in collagen deposition surrounding the ducts of the Cre-positive glands (blue staining) (Fig. 3C,D). To help determine the identity of the cells in the periductal stroma, we performed immunohistochemical staining for F4/80, a macrophage marker. This revealed a marked increase in macrophages in the periductal stroma in approximately 50% of the SmoM2;Cre glands (Fig. 3F) as compared to SmoM2;+ controls (Fig. 3E). Taken together, these data indicate that SmoM2 expression in the mammary epithelium results in alterations in the mammary gland stromal microenvironment.

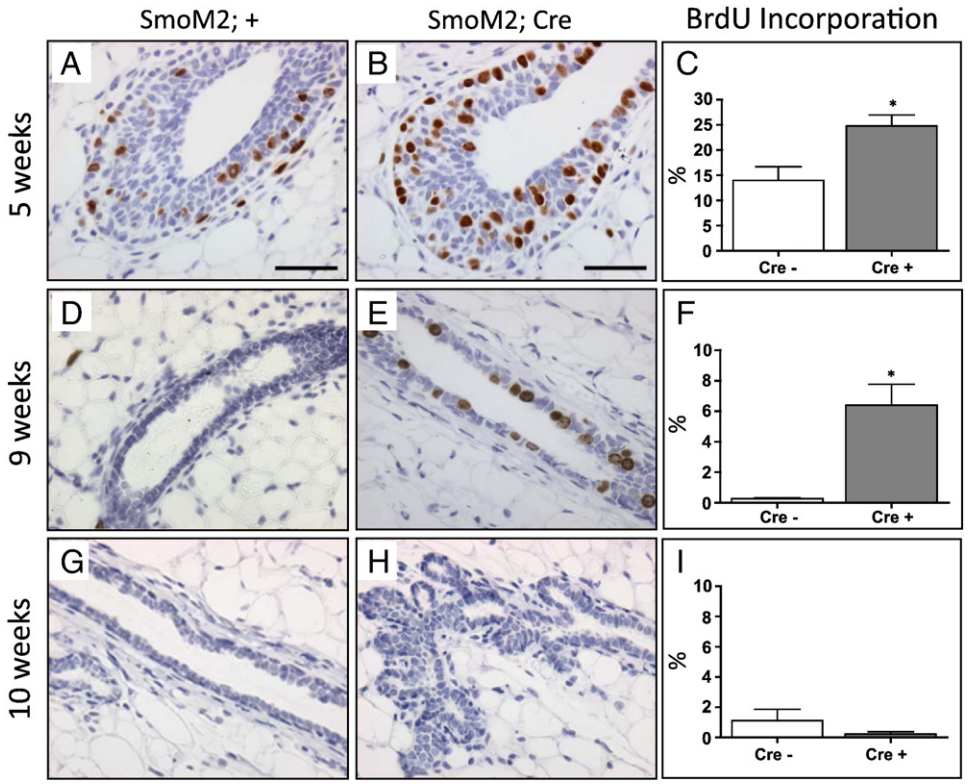

Fig. 2. SmoM2 expression leads to increased proliferation in the developing mammary gland. Immunohistochemistry for BrdU in paraffin embedded mammary gland sections from SmoM2;+ (A,D,G) and SmoM2;Cre (B,E,H) animals at 5, 9 and 10 weeks of age. SmoM2;Cre animals exhibit an increase in proliferation in the TEB's at 5 weeks of age ($p = 0.03$) (C) that persists until 9 weeks of age ($p < 0.01$) (F). By 10 weeks of age, the level of proliferation between SmoM2;Cre and SmoM2;+ littermates is not significantly different (I). Scale bars: 100 μm.

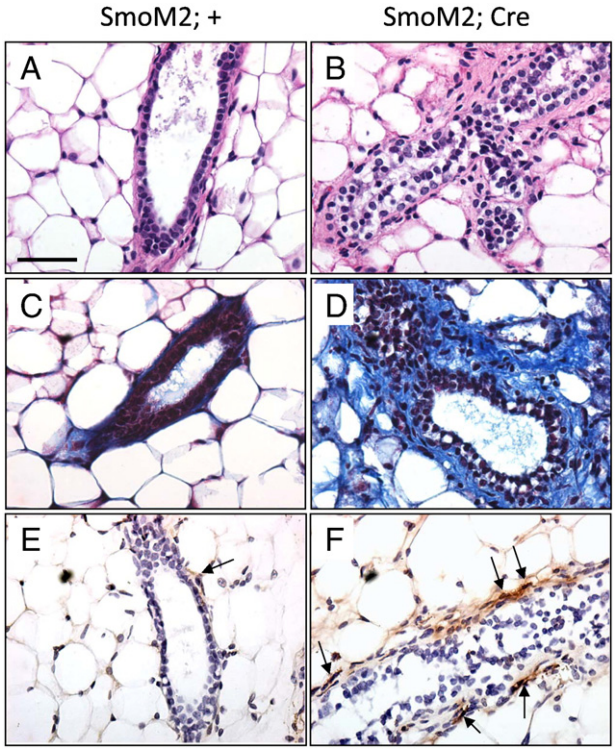

Fig. 3. SmoM2 expression leads to histological changes in the mammary gland epithelium and stroma. H&E (A,B) and Masson's Trichrome (C,D) staining of SmoM2;+ and SmoM2;Cre mammary gland sections. F4/80 immunostaining for macrophages in SmoM2;+ (E) and SmoM2;Cre (F) mammary gland sections. Arrows denote positive staining. Scale bars A–F: 100 μm.

SmoM2 expression is required in the luminal epithelium, but not in the myoepithelium for the observed mammary gland defects

In order to study the effect of SmoM2 expression in different cell types in the mammary gland, we employed adenoviral-Cre (Ad-Cre) infection *in vitro* on freshly isolated MECs from SmoM2;+ mice followed by subsequent transplantation. First SmoM2 mice were crossed to the R26R line, a lacZ reporter for Cre expression. MECs from SmoM2; R26R animals and R26R animals as a control were obtained and transduced with Ad-Cre to induce recombination. Ad-Cre elicits recombination in multiple cell types including stem and lineage-restricted progenitor cells. As a result, chimeric outgrowths containing recombined and un-recombined areas, as well as outgrowths in which only luminal or myoepithelial cell-types underwent recombination were obtained. Every outgrowth from the Ad-Cre treated SmoM2 MECs (8/8) was either hyper-branched and budded, or displayed aberrant TEB structures, or in some cases both phenotypes. A representative example of the outgrowths obtained is shown in Fig. 4. Control R26R outgrowths appeared normal and exhibited radial outgrowth as well as a moderate level of side branching (Fig. 4A,B). In contrast, SmoM2;R26R outgrowths exhibited hyper-branching and budding and also appeared disorganized (Fig. 4C,D). A chimeric SmoM2;R26R outgrowth is depicted in Fig. 4E. Recombined areas of the outgrowth (illustrated by the blue X-gal staining) showed hyper-branching and budding as compared to the un-recombined (dashed box) confirming that only areas containing SmoM2 expressing cells exhibit the hyper-branched phenotype observed. Significantly, areas of the outgrowths consisting of only a recombined myoepithelial cell layer with un-recombined luminal epithelium (observed in multiple ducts from three independent outgrowths) did not display the

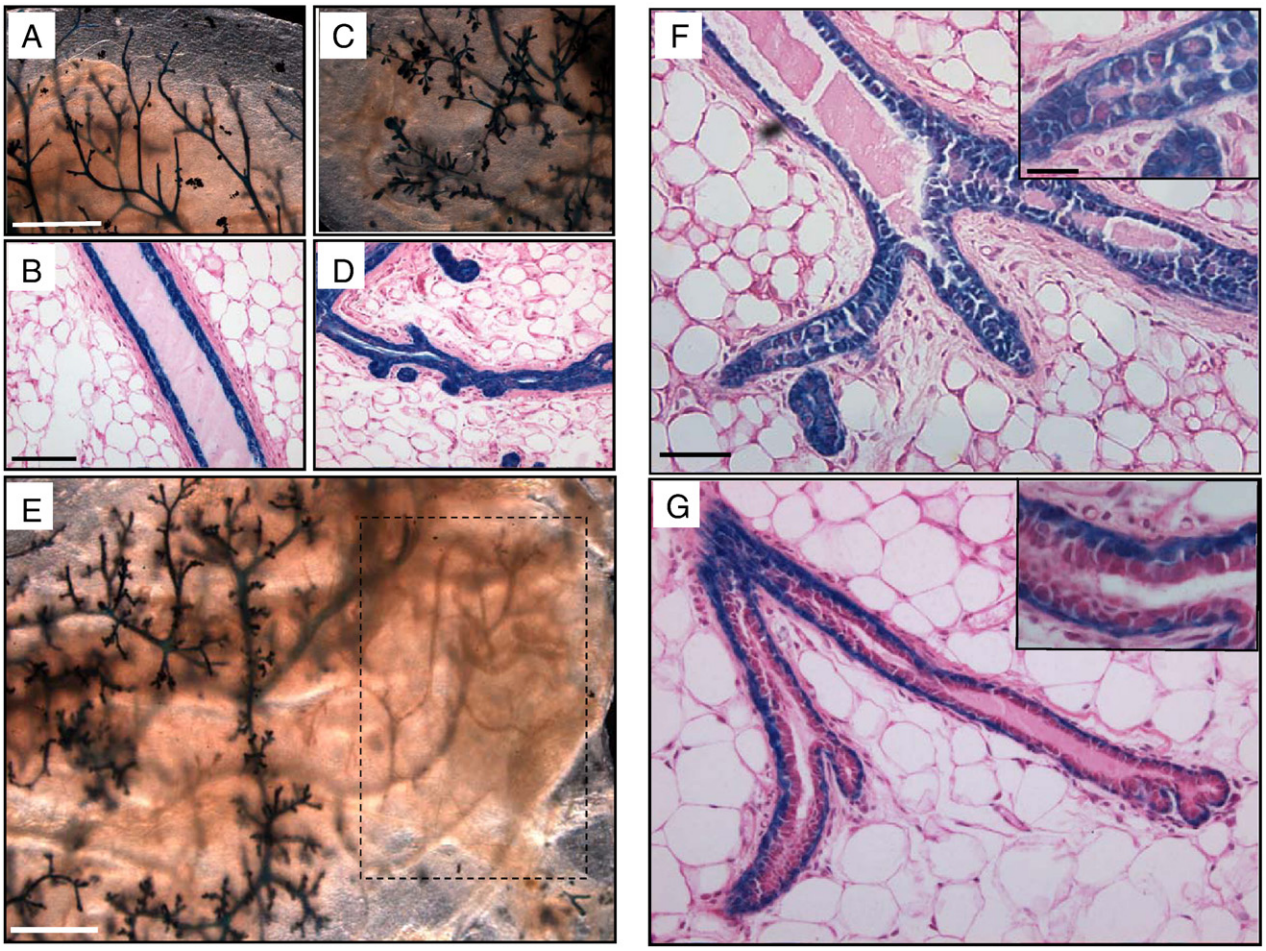

Fig. 4. Mammary gland reconstitution experiments after Ad-Cre treatment reveal a requirement for SmoM2 in luminal epithelium. X-gal stained whole-mounts and H&E sections of mammary gland outgrowths from R26R (A,B) and SmoM2;R26R (C–G) MECs illustrating how SmoM2 expressing cells participate in the hyper-branching phenotypes observed. Panel G illustrates an outgrowth in which only the myoepithelial cell layer underwent recombination. Scale bars: A,C,E 5 mm; B,D 100 μm; F,G 50 μm; Insets 20 μm.

hyper-branched and budded phenotype (Fig. 4G). Thus, SmoM2 expression in the luminal epithelium is required for the formation of the hyper-branched and budded mammary ductal trees and the changes in luminal, myoepithelial and periductal histology as illustrated in Fig. 4F.

The ductal hyperplasia phenotype requires interactions between SmoM2-expressing and wild type cells

In order to examine the consequences of activated Smo in SmoM2-expressing cells, non-expressing cells, and the surrounding environment more effectively, we crossed the SmoM2 animals to mice carrying a dual fluorescent reporter for Cre activity targeted to the Rosa26 locus (mT-mG). Cells in which SmoM2 is activated by Cre-mediated recombination express Cre-dependent EGFP, while cells in which SmoM2 is not activated by recombination remain Tomato Red-positive. Fluorescent imaging of whole mammary glands indicated that neither Cre-negative control mice (Fig. 5A) nor Cre-positive mice lacking the conditional SmoM2 allele (Fig. 5B) showed evidence of hyperplasia. In contrast, SmoM2;Cre mice exhibiting recombination (EGFP expression) showed hyper-branching and budding of the mammary ductal tree (Fig. 5C). However, areas of the mammary glands that exhibited 100% recombination did not display the hyperplastic phenotype (Fig. 5D–F). The hyper-branched and budded phenotype was only present in chimeric outgrowths containing both recombined (SmoM2-expressing) and un-recombined cells (Fig. 5G–I). These results demonstrate that wild type cells are required in order for the hyper-branching to occur, and further suggest that this phenotype is dependent upon either a paracrine or juxtacrine cell–cell interaction between the SmoM2 expressing cells and nearby wild type cells.

SmoM2-expressing cells stimulate the proliferation of neighboring wild type cells in a paracrine or juxtacrine manner

To demonstrate whether SmoM2 expressing cells stimulate proliferation of wild type cells in a paracrine or juxtacrine manner, we employed intraductal Ad-Cre delivery to activate SmoM2 and EGFP expression, with contralateral injection of adenoviral-LacZ as a negative control. This technique allowed us to achieve SmoM2 expression *in situ* in only a subset of cells, and to examine the effects on surrounding cells at specific times after SmoM2 expression. Two weeks after injections, the glands were harvested following a two-hour BrdU pulse and processed for staining. Co-staining for EGFP and BrdU revealed a significant increase in proliferation in cells surrounding SmoM2 expressing (EGFP positive) cells (Fig. 6A). Quantification of the staining (Fig. 6B) demonstrated that 14% ($\pm$4.1%) of the cells exhibited recombination (as determined by EGFP expression) in Ad-Cre treated ducts and Ad-lacZ treated ducts exhibited no recombination. Ad-Cre treated ducts showed a significant increase in BrdU incorporation ($2.91 \pm 0.8\%$) as compared to Ad-lacZ treated ducts ($0.21 \pm 0.1\%$) ($p = 0.01$). Significantly, in Ad-Cre treated ducts, the majority of proliferation occurred in un-recombined cells ($2.67 \pm 0.73\%$), but not in EGFP expressing cells

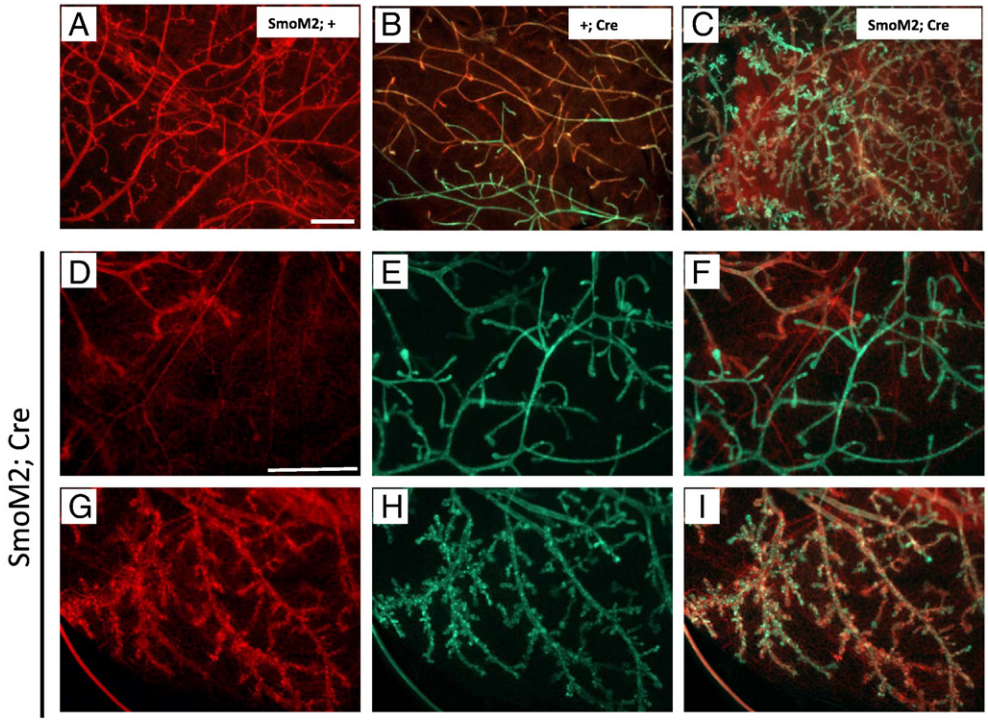

Fig. 5. Tagged SmoM2;Cre mammary glands exhibit hyper-branching and budding and reveal a possible requirement for SmoM2–wildtype cell interactions. Fluorescent images of whole glands from SmoM2;Cre and SmoM2;+, and +;Cre mammary glands illustrating un-recombined (Tomato Red+) and recombined (EGFP+) areas of the glands. Recombined cells marked by reporter EGFP expression have SmoM2 transgene expression. Merged image of a SmoM2;+ mammary gland (A). Merged image of a wild type; Cre positive mammary gland illustrating that EGFP expression alone is not responsible for the observed phenotypes (B). Merged image of a SmoM2;Cre mammary gland (C). Red, green, and merged images of sections from the same SmoM2;Cre mammary gland illustrating the requirement for un-recombined (Tomato Red+) cells in order for the presence of the hyper-branching phenotype (D–I). Scale bars A–C: 5 mm D–I: 5 mm.

(0.24 ± 0.05%) ($p<0.01$). These results indicate that SmoM2 cells are stimulating the proliferation of the surrounding wildtype cells while not significantly increasing proliferation in the SmoM2 expressing cells themselves. It is important to note that within Ad-Cre treated ducts, the increase in proliferative un-recombined (Tomato Red+) cells was only observed in those ducts containing at least one recombined (EGFP+) cell (Fig. S3), indicating that the proliferative stimulus from the SmoM2 cells requires either a close proximity or direct contact with wildtype cells.

SmoM2-expressing cells exhibit increased Hh signaling activity and possible downregulation of Notch pathway activity

In previously published models of Hh signaling activation in the mammary gland, the hallmark transcriptional targets of high level Hh signaling were not detected (Moraes et al., 2009, 2007). Several studies have suggested that canonical Hh signaling must be kept in a repressed state for normal virgin mammary gland development to occur (Hatsell and Cowin, 2006). In order to determine if SmoM2

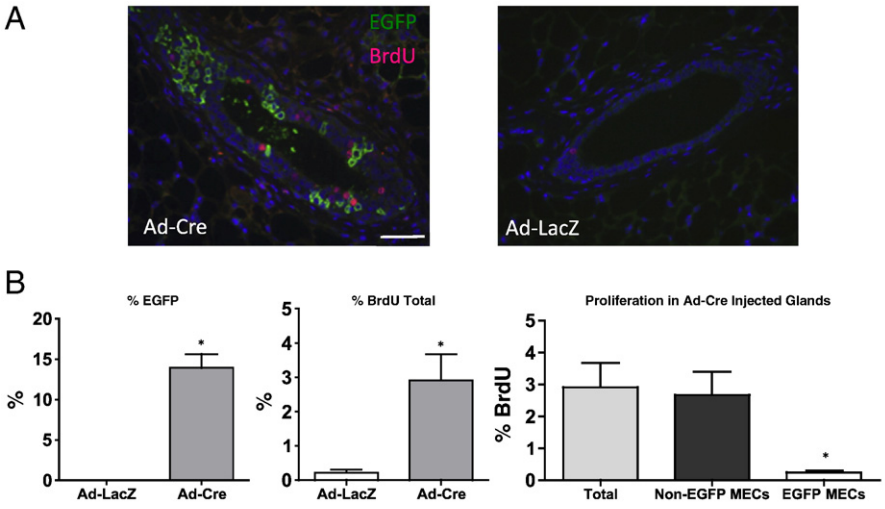

Fig. 6. SmoM2 expression stimulates proliferation of neighboring wildtype cells. Co-immunostaining for EGFP and BrdU in contralaterally injected inguinal mammary glands (A). The right side (4R) was injected with Ad-Cre and the left side (4L) was injected with Ad-LacZ as control. Ad-Cre injected glands exhibited 14% ± 4.1% EGFP expression, a marker for recombination and SmoM2 expression. Ad-Cre injected glands had a significant ($p = 0.01$) increase in the number of cells expressing BrdU as compared to Ad-LacZ injected control glands. The majority of proliferating cells (BrdU positive) were un-recombined cells (2.67 ± 0.73%) as compared to 0.24 ± 0.05% of BrdU positive EGFP expressing cells (B).

expression could elicit a canonical Hh transcriptional response, we took advantage of our tagged mouse model to sort recombined (EGFP) and un-recombined (Tomato Red) MEC populations from SmoM2;Cre mice and wildtype MECs from SmoM2;+ littermates (Fig. 7A). Total RNA was isolated from epithelial-enriched cell populations and qPCR was performed. As expected, SmoM2 transgene expression was increased 13-fold (±4.8) in EGFP-positive SmoM2:Cre MECs compared to the un-recombined Tomato Red-positive population (Fig. 7B). Fig. 7C illustrates the gene expression of the Hh signal pathway components in all three sorted cell populations. An induction of Gli2 (18±7.2 fold change $p=0.03$) expression as well as a marked increase of Gli1 (71±24.2 fold change $p=0.04$) and Ptch2 (55±20.3 fold change $p=0.04$) was observed in EGFP+ (recombined) SmoM2;Cre MECs as compared to SmoM2;+ cells. An induction (5±0.9 fold) in Gli2 was observed in Tomato Red+ (un-recombined) cells. Additionally, and induction of Smo expression was observed in both recombined (EGFP+) and un-recombined (Tomato Red+) cells from SmoM2;Cre mice as compared to cells from Cre negative litter-mates. These data indicate that activation of canonical Hh signaling occurred in the SmoM2 expressing cells.

Since SmoM2-expressing cells were stimulating proliferation of wildtype cells adjacent or in-close proximity, we next investigated whether expression of members of the Notch signaling pathway, which is known to function in a juxtacrine manner, was altered. Fig. 7D illustrates the gene expression patterns of several Notch pathway members in all three sorted cell populations. A marked upregulation of the Notch ligands delta-like 1 (Dll-1), (21±6.8 fold change $p=0.02$) and Jagged-2 (Jag2) (5±1.0 fold change $p<0.01$) was detected in EGFP+ (recombined) cells from SmoM2;Cre mice, as compared to wildtype MECs from SmoM2;+ mice. Additionally, the Notch 4 receptor (18±11.9 fold change $p<0.01$) along with the Hes6 target gene (7±3.7 fold change $p=0.03$) and the Delta-like 4 (Dll4) ligand (14±9.1 fold change $p<0.01$) were found to be downregulated in the EGFP-positive cell population. The Notch1 receptor was found to be slightly upregulated (less than 1 fold) in both EGFP and TomatoRed populations. No significant changes were observed in other pathway members tested.

Epithelial SmoM2 expression disrupts luminal–myoepithelial cell interactions and alters luminal epithelial cell differentiation

In order to determine if the morphological changes observed after SmoM2 expression were due to aberrant differentiation and organization of distinct mammary epithelial cell subtypes, we examined the luminal and myoepithelial cell layers by immunostaining with antibodies that detect keratin 8 (K8), a luminal cell marker and keratin 14 (K14), a myoepithelial cell marker (Fig. 8). While both of these markers were readily detected in SmoM2;Cre glands, the typical bilayer of ductal epithelium was disrupted as compared to SmoM2;+ controls. Furthermore, K14-expressing cells were rounded as opposed to their characteristic elongated shape (Fig. 8B), and appeared dissociated from the luminal cells and possibly from the basement membrane (Fig. 8A vs. 8B and insets). In this trigenic model, recombination and SmoM2 expression (as measured by EGFP detection) occurs in both luminal and myoepithelial cell layers (Fig. S4).

In order to determine if the dissociation of the mammary gland bilayer was due to expression of SmoM2 in the myoepithelial cell layer, we examined K8-K14 expression in SmoM2/mT-mE glands injected intraductally with Ad-Cre. Serial sections were stained for

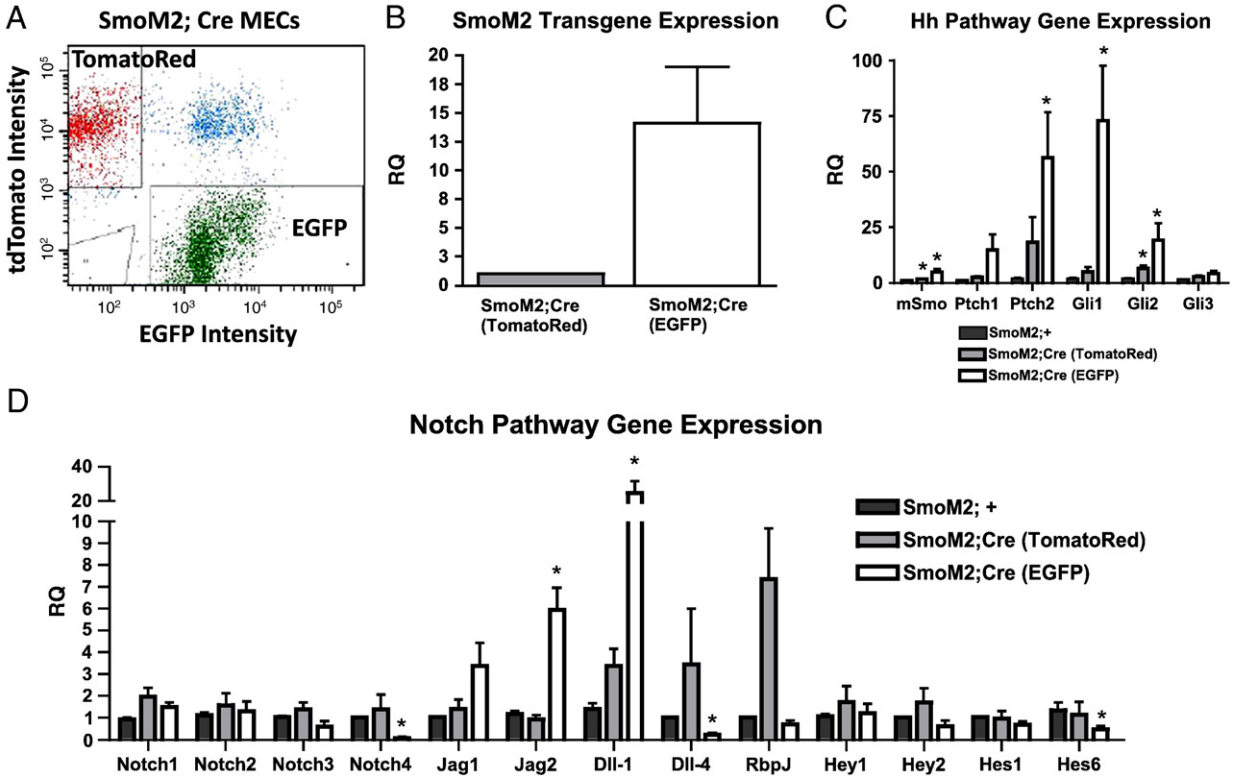

Fig. 7. SmoM2 expressing cells have active Hh signaling and downregulation of the Notch pathway. Representative FACS plot illustrating EGFP expressing (recombined) SmoM2;Cre MECs and Tomato Red expressing (un-recombined) SmoM2;Cre MEC populations (A). Quantitative RT-PCR illustrating the 13-fold increased expression of SmoM2 ($p=.03$) in EGFP expressing (recombined) SmoM2;Cre MECs as compared to Tomato Red expressing (un-recombined) SmoM2;Cre MECs (B). Hh pathway gene expression in sorted cell populations illustrating induction of Ptch2 ($p=0.04$), Gli-1 ($p=0.04$), and Gli-2 ($p=0.03$) in EGFP expressing (recombined) SmoM2;Cre MECs as compared to wildtype SmoM2;+ MECs (C). Notch pathway gene expression in sorted cell populations illustrating the 23-fold increased expression of Dll-1 ($p=0.02$), the 5-fold increased expression of Jag2 ($p<0.01$), and the 18-fold downregulation of Notch4 ($p<0.0001$), the 14-fold downregulation of Dll-4 ($p=0.03$) and the 7-fold downregulation of Hes6 ($p=0.03$) in EGFP expressing (recombined) SmoM2;Cre MECs as compared to wildtype SmoM2;+ MECs.

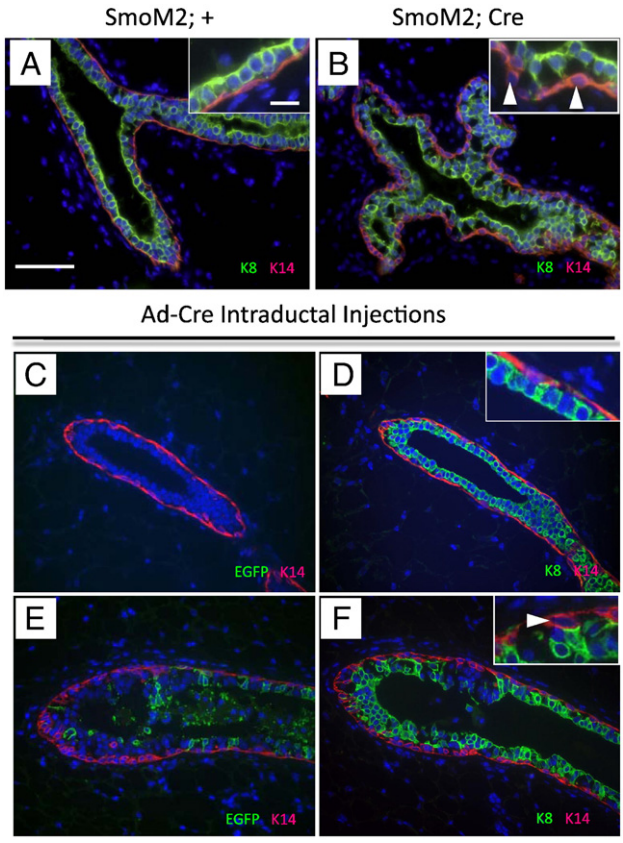

Fig. 8. SmoM2 expression leads dissociation between the luminal and myoepithelial cell layers. Co-immunostaining for luminal marker kertain-8 (K8) and myoepithelial cell marker keratin-14 (K14) in SmoM2;+ (A) and SmoM2;Cre (B) mammary glands. Mammary glands from SmoM;Cre mice exhibit dissociation of the luminal and myoepithelial cell layer (B) and altered morphology of the myoepithelial cells (B inset) as compared to Cre negative litter-mates (A). Co-immunostaining for EGFP (as a marker for SmoM2 expression) and K14 (C,E) and K8-K14 (D,F) in serial sections from mammary glands from SmoM2/mTmG mice intraductally injected with Ad-Cre. The dissociation of the luminal and myoepithelial cell layers was not observed in ducts lacking EGFP expression (C,D) and only present in ducts with luminal EGFP expression (E,F). Insets are magnifications depicting the luminal and myoepithelial cell interface. Arrows indicate K14 positive cells that have lost their characteristic elongated shape. Scale bars A–F: 75 μm Insets: 10 μm.

EGFP and K-14 expression (Fig. 8C,E) and K8 and K-14 expression (Fig. 8D,F) in order to examine the bilayer interaction in areas with low or no recombination as well as in areas with high levels of SmoM2 expression. Disruption of the luminal and myoepithelial cell layers was only apparent in ducts containing EGFP expression in luminal cells (Fig. 8E,F) as compared to ducts containing no EGFP expression (Fig. 8C,D). Ad-lacZ injected glands exhibited the normal pattern of K8 and K14 expression and typical bilayer interaction and appeared indistinguishable from the Ad-Cre injected ducts with no EGFP expression (Fig. S5). Since recombination in the Ad-Cre injected glands occurs primarily in the luminal epithelium (Fig. S6), it is likely that SmoM2 transgene expression in only the luminal compartment is sufficient for the observed phenotypes.

To examine the proper differentiation of luminal epithelial cells further, particularly with respect to hyperplastic alveolar buds, we performed immunostaining for a specific marker for the transition from luminal to alveolar cells. The Na–K–Cl co-transporter-1 (NKCC1) is normally expressed throughout the differentiated luminal epithelium of virgin mammary glands and is absent in alveolar cells during pregnancy (Shillingford et al., 2002). SmoM2;Cre mammary glands showed loss of NKCC1 expression in a large percentage of cells as compared to SmoM2;+ littermates (Fig. 9A,B). This loss of expression occurred not only in the alveolar-like cells as seen during pregnancy, but also throughout the ductal epithelium in virgin mice. We also examined NKCC1 expression in Ad-Cre and Ad-LacZ injected glands and found that in comparison to Ad-LacZ treated glands (Fig. 9C) this marker again was absent in Ad-Cre injected glands predominantly in SmoM2 (EGFP+) cells (Fig. 9D). Arrows illustrate regions of the duct in which NKCC1 expression is absent.

Despite these changes in differentiation, no detectable changes in the expression or distribution of estrogen receptor (ER) or progesterone receptor (PR) were observed (data not shown). Therefore, these studies suggest that although SmoM2;Cre glands still maintain a distinct luminal and myoepithelial cell identity as well as normal levels of hormone receptors, SmoM2 expression in the luminal epithelium is sufficient to cause altered luminal cell differentiation and disrupted interactions between the luminal and myoepithelial cell layers.

Discussion

In this study, we report that SmoM2 expression in luminal mammary epithelium, but not myoepithelium, leads to increased proliferation as well as to defects in mammary gland morphology. Developmental defects are associated with changes in luminal–myoepithelial cell–cell interactions as well as to altered epithelial–stromal tissue interactions. Using genetically tagged mammary gland chimeras, as well as adenoviral induced chimeras, we show that SmoM2 expressing cells are capable of stimulating proliferation in neighboring wild type cells, demonstrating that either a paracrine or juxtacrine mechanism may be responsible for the observed effects. Finally, we show that SmoM2 expression leads to an upregulation of the canonical Hh transcription factors Gli1 and Gli2 as well as to upregulation of the canonical target Ptch2. Additionally, SmoM2 expression leads to upregulation of notch pathway ligands Dll-1, and Jag2, as well as to downregulation of the notch pathway receptor Notch4 and of target gene Hes6, suggesting a cooperation of these two pathways in eliciting the observed phenotypes.

Stimulation of proliferation by SmoM2 expressing cells

Previous analysis of SmoM2 expression in the mammary gland showed alterations in mammary gland morphology and increased proliferation (Moraes et al., 2007). However, while results suggested that paracrine cell–cell interactions might be responsible for the observed proliferative phenotype, this hypothesis could not be formally tested using available models. In this study, we were able to generate adenoviral induced tagged chimeras that allowed us to demonstrate conclusively that SmoM2 expression stimulated proliferation of surrounding wildtype cells. The adenoviral-induced chimeras have the advantage that they produce ducts with both recombined and un-recombined cells in the same mammary gland. Furthermore, an adenovirus lacking the Cre recombinase can be injected in the same mouse facilitating a comparison with the contralateral mammary gland, thus providing ideal controls for any systemic effects. Our observations that hyper-proliferation in response to SmoM2 cells only occurred in ducts containing recombined cells and that 50% of proliferating cells observed were in direct cell contact with a SmoM2 expressing cell, provide strong evidence for either a short range paracrine- or juxtacrine-mediated effect. Although many reports of induced proliferation resulting from the canonical activation of the Hh pathway exist, we now demonstrate that this effect can be non-cell autonomous — a possibility that cannot generally be easily tested in most other developmental models.

Increased expression of Ptch2, Gli1, and Gli2

In previously published models of Hh signaling activation in the mammary gland, the hallmark transcriptional targets of high level Hh

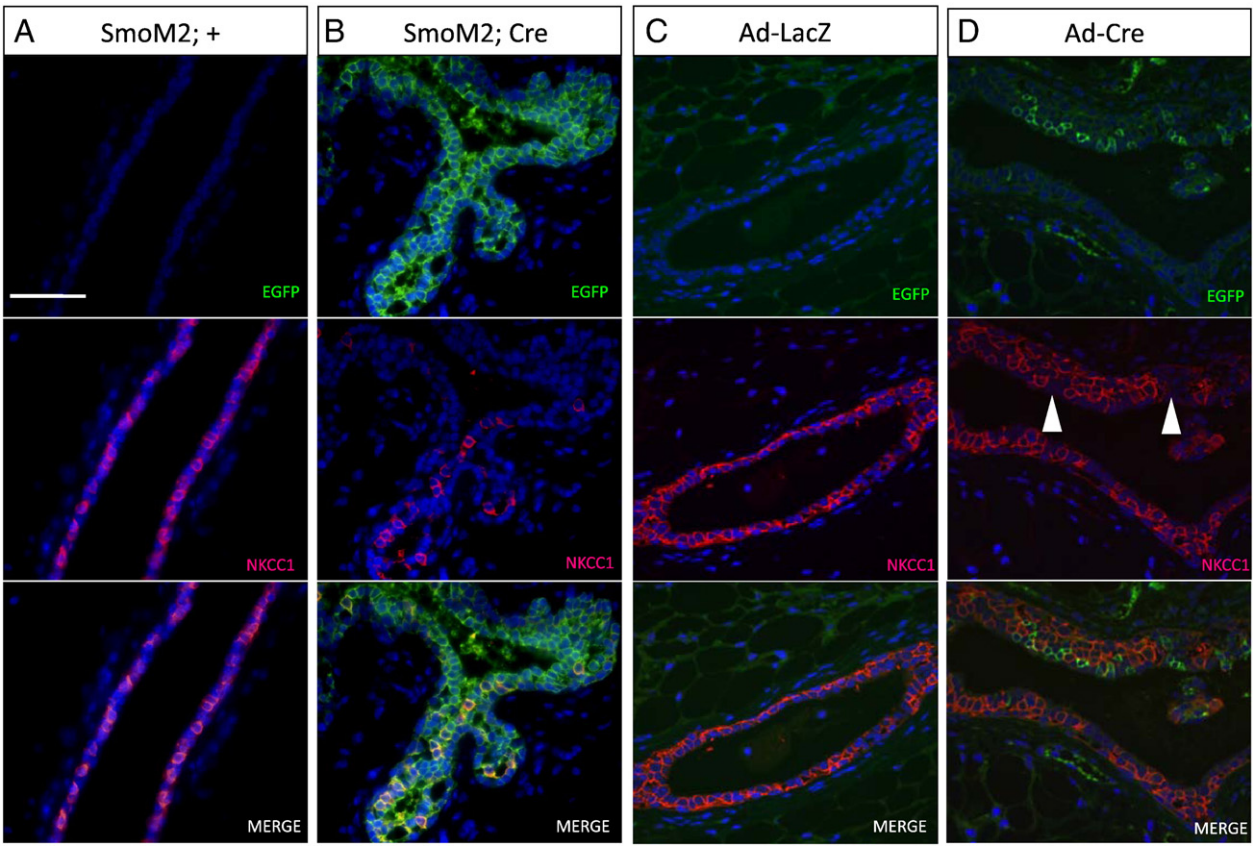

Fig. 9. SmoM2 expression leads to changes in luminal epithelial cell identity. Single channel and merged images of co-immunostaining for EGFP and NKCC1 in SmoM2;+ (A), SmoM2;Cre (B) and in SmoM2/mTmE glands intraductally injected with Ad-LacZ (C) and Ad-Cre (D). NKCC1 expression was not detected in a large population of cells in mammary glands from SmoM2;Cre mice relative to litter-mate controls. In glands injected intraductally with Ad-Cre, NKCC1 was not detected predominantly in EGFP expressing cells (arrows). Scale bars A–F: 50 μm.

signaling were not detected (Moraes et al., 2009, 2007). Using our tagged model we were able to analyze gene expression in SmoM2 expressing and surrounding wildtype cells selectively. We demonstrated a robust activation of the canonical Hh pathway as revealed by Gli1 and Gli2 upregulation as well as upregulation of the Ptch2 receptor in SmoM2 expressing cells. The discrepancy between the models appears to be due to masking of the transcriptional response when using total mammary gland RNA representing both epithelial and stromal cells. In support of this interpretation, following RNA isolation from the total mammary gland we only detected a two-fold increase in Gli1 expression with the conditional SmoM2 model (Fig. S7), whereas in the FACS purified SmoM2 expressing cells we detected a 71-fold increase in Gli1 and an 18-fold increase in Gli2.

With respect to Gli1, Gli1 overexpression in the virgin mammary epithelium did not result in a detectable phenotype. Lack of a demonstrable phenotype was attributed to low transgene expression at this stage of development (Fiaschi et al., 2007). However, during pregnancy and lactation the transgene was detectable leading to failure of differentiation during pregnancy and defective lactation. Pregnancy associated proliferation was increased and recruitment of periductal macrophages was also reported, similar to our observations in virgin mice.

Upregulation of Notch pathway ligands Dll-1 and Jag-2 and downregulation of Notch pathway receptor Notch4 and target gene Hes6

The observed increase in Dll-1 and Jag2 in MECs that over expressed SmoM2 has several possible implications. Notch signaling in the mammary gland has been shown to promote luminal cell fate determination and repress mammary stem cell expansion *in vivo* (Bouras et al., 2008; Yalcin-Ozuysal et al., 2010), both of which are observed in SmoM2 overexpressing mouse models ((Moraes et al., 2007) and this work). Additionally, activated Notch signaling has also been shown to elicit a graded response in human mammary epithelial cells. Low Notch activity stimulated a hyper-proliferative response, while high Notch activity caused downregulation of matrix-adhesion genes and inhibition of proliferation (Mazzone et al., 2010). Since increased ligand expression can stimulate Notch pathway activity transiently in the surrounding cells, and also down regulate Notch activity in the signaling cell via cis-inactivation (consistent with our observation of Notch4 and Hes6 downregulation in the SmoM2 expressing cell population), this model of Notch pathway activity might explain the hyper-proliferative response observed in wildtype cells surrounding SmoM2 expressing cells. Furthermore Dll1, which has been historically considered solely as a Notch receptor ligand, was recently shown to have signaling properties when cleaved and bind to the Smad family of proteins to modulate transcription of genes downstream of the TGF-β/Activin pathway (Hiratochi et al., 2007). TGF-β signaling has been shown to act as a negative signal for proliferation in the mammary gland and to restrict branching morphogenesis (Sternlicht, 2006). This mechanism may account for the failure to observe proliferation of SmoM2-expressing cells, and furthermore explain why proliferation levels in SmoM;Cre glands revert to normal at ten weeks of age. The only discrepancy to the proposed model is the observed transcriptional downregulation of the Dll-4 ligand in the SmoM2 expressing cell population. Although surprising due to the marked upregulation of the other ligands, this observation may be explained by data indicating that Notch ligands can exert opposing roles. It is well documented that Dll-4 and Jag1 can exert opposing roles during vascular development (Benedito et al.,

2009). If this is the case in the mammary gland, it is likely that upregulation of some ligands can in-turn produce downregulation of others.

Alterations in cell differentiation and disruption of luminal–myoepithelial cell interactions

Myoepithelial cells have been shown to modulate epithelial–stromal interactions and to actively participate in the composition and organization of the extracellular matrix (ECM) (Faraldo et al., 2005). It is possible that the stromal phenotypes observed in these studies are a direct result of SmoM2 expression in myoepithelial cells. However, evidence from the mammary gland chimeras obtained in the transplantation studies would argue that this effect must be indirect from the luminal epithelial cells since SmoM2 expression in the myoepithelial cell layer alone was insufficient to elicit the observed stromal defects. This finding suggests that either myoepithelial cells are not competent to transduce the SmoM2 signal, or that they are unable to relay a secondary signal following SmoM2 expression. Another possibility is that the effects seen in the stroma are due to the observed dissociation between luminal and myoepithelial cells. Myoepithelial cells mediate the cross talk between luminal cells and the stroma and these interactions are thought to be required for appropriate growth, branching and differentiation of the mammary gland (Faraldo et al., 2005). If this cross-talk were disrupted as a result of SmoM2 expression in luminal cells and their dissociation from myoepithelial cells, then the tight control required to regulate the appropriate amount of side branching and ECM components might be altered.

NKCC1 expression has traditionally been associated with a differentiated luminal cell fate and is lost in cells that transition to an alveolar cell fate during pregnancy. The fact that loss of NKCC1 occurs throughout the gland in the trigenic animals and not exclusively in the alveolar like buds as it occurs during pregnancy is an interesting observation. Additionally, in the adenoviral induced chimeric model, loss of NKCC1 is only apparent in ducts containing recombined cells and appears to be primarily lost in SmoM2 expressing cells, suggesting that it is a cell-autonomous effect. When these results are considered in the context of Notch pathway activity and its role in promoting luminal cell fate determination, they support a hypothesis in which a decrease in Notch pathway activity in SmoM2 expressing cells, as evidenced by loss of Notch4 and Hes6 expression and high expression of Dll-1 and Jag2 ligands, might account for this apparent change in cell differentiation. Thus, if SmoM2 expressing cells are no longer able to maintain a fully differentiated luminal cell fate, this might account for their loss of NKCC1 expression. This hypothesis might also explain previous observations of increased mammary gland progenitor cells following SmoM2 expression (Moraes et al., 2007).

Conclusions and other considerations

In conclusion, SmoM2 expression in the mammary gland appears to exert both cell-autonomous and non-cell autonomous effects. While it is able to stimulate the proliferation of wildtype MECs as well as to alter their morphology and myoepithelial–luminal cell organization, this process appears to be tightly regulated and may be influenced by a negative feedback mechanism (e.g. TGF-β signaling). Furthermore, SmoM2 expression in the mammary epithelium results in changes in the mammary gland microenvironment.

Despite the proliferative effects and the changes in histoarchitecture observed in SmoM2 expressing glands, these do not progress to form tumors at a higher rate than that observed in wild type mice. While SmoM2 expression alone might not be sufficient to elicit a tumor phenotype, it might provide the appropriate environment in which to acquire a second hit in the transformation from normal to tumor. This hypothesis is being tested explicitly in our laboratory. Evidence from other models of Hh activation supports the hypothesis that activation of Hh signaling alone might not be sufficient to induce mammary tumorigenesis. SmoM2 expression under the control of the MMTV promoter failed to show an increase in tumor formation (Moraes et al., 2007). Additionally, long-term tumor formation studies in *Ptch1* heterozygotes did not show increased frequency of mammary tumors (Goodrich et al., 1997). Finally, targeted mammary gland overexpression of Gli1 produced tumors, but only after multiple pregnancies, suggesting that Gli1 expression alone is not sufficient to elicit mammary tumors (Fiaschi et al., 2009). These observations are in agreement with human breast cancer data where Smo is highly expressed in approximately 70% of ductal carcinomas *in situ*, early breast cancer lesions, but only over-expressed in about 30% of invasive breast cancers.

Supplementary materials related to this article can be found online at doi:10.1016/j.ydbio.2011.01.025.

Acknowledgments

We would like to thank Dr. Timothy Lane for kindly providing the MMTV-Cre line. We would like to thank Shirley Small and John Landua for help with mouse colony maintenance and Amy Shore for helpful discussion. This work was supported by grants from the National Institutes of Health to M.T.L. (P01-CA30195 and R01-CA127857), J.M.R (R37-CA16303), and Y.L. (R01-CA124820). A.P.V. was supported by a Department of Defense Pre-doctoral Fellowship Award (W81XWH-06-1-0707).

References

Benedito, R., Roca, C., Sorensen, I., Adams, S., Gossler, A., Fruttiger, M., Adams, R.H., 2009. The notch ligands Dll4 and Jagged1 have opposing effects on angiogenesis. Cell 137, 1124–1135.

Bouras, T., Pal, B., Vaillant, F., Harburg, G., Asselin-Labat, M.L., Oakes, S.R., Lindeman, G.J., Visvader, J.E., 2008. Notch signaling regulates mammary stem cell function and luminal cell-fate commitment. Cell Stem Cell 3, 429–441.

Chari, N.S., McDonnell, T.J., 2007. The sonic hedgehog signaling network in development and neoplasia. Adv. Anat. Pathol. 14, 344–352.

Daniel, C.W., Silberstein, G.B., Van Horn, K., Strickland, P., Robinson, S., 1989. TGF-beta 1-induced inhibition of mouse mammary ductal growth: developmental specificity and characterization. Dev. Biol. 135, 20–30.

Deome, K.B., Faulkin Jr., L.J., Bern, H.A., Blair, P.B., 1959. Development of mammary tumors from hyperplastic alveolar nodules transplanted into gland-free mammary fat pads of female C3H mice. Cancer Res. 19, 515–520.

Evangelista, M., Tian, H., de Sauvage, F.J., 2006. The hedgehog signaling pathway in cancer. Clin. Cancer Res. 12, 5924–5928.

Faraldo, M.M., Teuliere, J., Deugnier, M.A., Taddei-De La Hosseraye, I., Thiery, J.P., Glukhova, M.A., 2005. Myoepithelial cells in the control of mammary development and tumorigenesis: data from genetically modified mice. J. Mammary Gland Biol. Neoplasia 10, 211–219.

Fiaschi, M., Rozell, B., Bergstrom, A., Toftgard, R., 2009. Development of mammary tumors by conditional expression of GLI1. Cancer Res. 69, 4810–4817.

Fiaschi, M., Rozell, B., Bergstrom, A., Toftgard, R., Kleman, M.I., 2007. Targeted expression of GLI1 in the mammary gland disrupts pregnancy-induced maturation and causes lactation failure. J. Biol. Chem. 282, 36090–36101.

Goodrich, L.V., Milenkovic, L., Higgins, K.M., Scott, M.P., 1997. Altered neural cell fates and medulloblastoma in mouse patched mutants. Science 277, 1109–1113.

Hatsell, S.J., Cowin, P., 2006. Gli3-mediated repression of Hedgehog targets is required for normal mammary development. Development 133, 3661–3670.

Hiratochi, M., Nagase, H., Kuramochi, Y., Koh, C.S., Ohkawara, T., Nakayama, K., 2007. The Delta intracellular domain mediates TGF-beta/Activin signaling through binding to Smads and has an important bi-directional function in the Notch–Delta signaling pathway. Nucleic Acids Res. 35, 912–922.

Jeong, J., Mao, J., Tenzen, T., Kottmann, A.H., McMahon, A.P., 2004. Hedgehog signaling in the neural crest cells regulates the patterning and growth of facial primordia. Genes Dev. 18, 937–951.

Jia, J., Jiang, J., 2006. Decoding the Hedgehog signal in animal development. Cell. Mol. Life Sci. 63, 1249–1265.

Kasper, M., Jaks, V., Fiaschi, M., Toftgard, R., 2009. Hedgehog signalling in breast cancer. Carcinogenesis 30, 903–911.

LaMarca, H.L., Visbal, A.P., Creighton, C.J., Liu, H., Zhang, Y., Behbod, F., Rosen, J.M., 2010. CCAAT/enhancer binding protein beta regulates stem cell activity and specifies luminal cell fate in the mammary gland. Stem Cells 28, 535–544.

Landua, J.D., Visbal, A.P., Lewis, M.T., 2009. Methods for preparing fluorescent and neutral red-stained whole mounts of mouse mammary glands. J. Mammary Gland Biol. Neoplasia 14, 411–415.

Lewis, M.T., Ross, S., Strickland, P.A., Sugnet, C.W., Jimenez, E., Hui, C., Daniel, C.W., 2001. The Gli2 transcription factor is required for normal mouse mammary gland development. Dev. Biol. 238, 133–144.
Li, G., Robinson, G.W., Lesche, R., Martinez-Diaz, H., Jiang, Z., Rozengurt, N., Wagner, K.U., Wu, D.C., Lane, T.F., Liu, X., Hennighausen, L., Wu, H., 2002. Conditional loss of PTEN leads to precocious development and neoplasia in the mammary gland. Development 129, 4159–4170.
Livak, K.J., Schmittgen, T.D., 2001. Analysis of relative gene expression data using real-time quantitative PCR and the 2(−Delta Delta C(T)) Method. Methods 25, 402–408.
Mazzone, M., Selfors, L.M., Albeck, J., Overholtzer, M., Sale, S., Carroll, D.L., Pandya, D., Lu, Y., Mills, G.B., Aster, J.C., Artavanis-Tsakonas, S., Brugge, J.S., 2010. Dose-dependent induction of distinct phenotypic responses to Notch pathway activation in mammary epithelial cells. Proc. Natl Acad. Sci. USA 107, 5012–5017.
McMahon, A.P., Ingham, P.W., Tabin, C.J., 2003. Developmental roles and clinical significance of hedgehog signaling. Curr. Top. Dev. Biol. 53, 1–114.
Moraes, R.C., Chang, H., Harrington, N., Landua, J.D., Prigge, J.T., Lane, T.F., Wainwright, B.J., Hamel, P.A., Lewis, M.T., 2009. Ptch1 is required locally for mammary gland morphogenesis and systemically for ductal elongation. Development 136, 1423–1432.
Moraes, R.C., Zhang, X., Harrington, N., Fung, J.Y., Wu, M.F., Hilsenbeck, S.G., Allred, D.C., Lewis, M.T., 2007. Constitutive activation of smoothened (SMO) in mammary glands of transgenic mice leads to increased proliferation, altered differentiation and ductal dysplasia. Development 134, 1231–1242.
Muzumdar, M.D., Tasic, B., Miyamichi, K., Li, L., Luo, L., 2007. A global double-fluorescent Cre reporter mouse. Genesis 45, 593–605.
Rijnkels, M., Rosen, J.M., 2001. Adenovirus-Cre-mediated recombination in mammary epithelial early progenitor cells. J. Cell Sci. 114, 3147–3153.
Russell, T.D., Fischer, A., Beeman, N.E., Freed, E.F., Neville, M.C., Schaack, J., 2003. Transduction of the mammary epithelium with adenovirus vectors in vivo. J. Virol. 77, 5801–5809.
Shillingford, J.M., Miyoshi, K., Flagella, M., Shull, G.E., Hennighausen, L., 2002. Mouse mammary epithelial cells express the Na–K–Cl cotransporter, NKCC1: characterization, localization, and involvement in ductal development and morphogenesis. Mol. Endocrinol. 16, 1309–1321.
Soriano, P., 1999. Generalized lacZ expression with the ROSA26 Cre reporter strain. Nat. Genet. 21, 70–71.
Sternlicht, M.D., 2006. Key stages in mammary gland development: the cues that regulate ductal branching morphogenesis. Breast Cancer Res. 8, 201.
Varjosalo, M., Taipale, J., 2008. Hedgehog: functions and mechanisms. Genes Dev. 22, 2454–2472.
Visbal, A.P., Lewis, M.T., 2010. Hedgehog signaling in the normal and neoplastic mammary gland. Curr. Drug Targets 11, 1103–1111.
Watson, C.J., Khaled, W.T., 2008. Mammary development in the embryo and adult: a journey of morphogenesis and commitment. Development 135, 995–1003.
Welm, B.E., Dijkgraaf, G.J., Bledau, A.S., Welm, A.L., Werb, Z., 2008. Lentiviral transduction of mammary stem cells for analysis of gene function during development and cancer. Cell Stem Cell 2, 90–102.
Yalcin-Ozuysal, O., Fiche, M., Guitierrez, M., Wagner, K.U., Raffoul, W., Brisken, C., 2010. Antagonistic roles of Notch and p63 in controlling mammary epithelial cell fates. Cell Death Differ 17, 1600–1612.